


Myeloid tumor necrosis factor and heme oxygenase-1 regulate the progression of colorectal liver metastases during hepatic ischemia-reperfusion

Desislava Germanova^{1,2} | Jiri Keirsse^{3,4} | Arnaud Köhler^{1,2} |
 Jean-François Hastir^{1,2} | Peter Demetter⁵ | Sandrine Delbauve^{1,2} |
 Yvon Elkrim^{3,4} | Laurine Verset⁵ | Lionel Larbanoix⁶ | Nicolas Preyat⁷ |
 Sophie Laurent⁶ | Sergei Nedospasov⁸ | Vincent Donckier⁹ |
 Jo A. Van Ginderachter^{3,4} | Véronique Flamand^{1,2} 

¹Institut d'Immunologie Médicale, Université Libre de Bruxelles, Belgium

²ULB Center for Research in Immunology (U-CRI), Belgium

³Laboratory of Cellular and Molecular Immunology, Vrije Universiteit Brussel, Brussels, Belgium

⁴Myeloid Cell Immunology Lab, VIB Center for Inflammation Research, Brussels, Belgium

⁵Department of Pathology, Erasme University Hospital, Université Libre de Bruxelles, Brussels, Belgium

⁶Center for Microscopy and Molecular Imaging, Université de Mons, Belgium

⁷Laboratory of Immunobiology, Université Libre de Bruxelles, Belgium

⁸Engelhardt Institute of Molecular Biology, Russian Academy of Sciences and Lomonosov Moscow State University, Moscow, Russia

⁹Service de Chirurgie, Institut Jules Bordet, Université Libre de Bruxelles, Brussels, Belgium

Correspondence

Véronique Flamand, Institut d'Immunologie Médicale, Université Libre de Bruxelles, Rue Adrienne Bolland, 8 6041 Gosselies, Belgium.
 Email: veronique.flamand@ulb.be

Funding information

Fonds De La Recherche Scientifique - FNRS, Grant/Award Number: Projet de recherche; Fonds pour la recherche médicale dans le Hainaut (FRMH), Grant/Award Number: research grant; Foundation against cancer, Belgium; The European Regional Development Fund and the Walloon Region; the Fonds Erasme research grant

Abstract

The liver ischemia-reperfusion (IR) injury that occurs consequently to hepatic resection performed in patients with metastases can lead to tumor relapse for not fully understood reasons. We assessed the effects of liver IR on tumor growth and the innate immune response in a mouse model of colorectal (CR) liver metastasis. Mice subjected to liver ischemia 2 days after intrasplenic injection of CR carcinoma cells displayed a higher metastatic load in the liver, correlating with Kupffer cells (KC) death through the activation of receptor-interacting protein 3 kinase (RIPK3) and caspase-1 and a recruitment of monocytes. Interestingly, the immunoregulatory mediators, tumor necrosis factor- α (TNF- α) and heme oxygenase-1 (HO-1) were strongly upregulated in recruited monocytes and were also expressed in the surviving KC following IR. Using TNF^{flox/flox} LysM^{cre/wt} mice, we showed that TNF deficiency in macrophages and monocytes favors tumor progression after IR. The antitumor effect of myeloid cell-derived TNF involved direct tumor cell apoptosis and a reduced expression of immunosuppressive molecules such as transforming growth factor- β , interleukin (IL)-10, inducible nitric oxide synthase (iNOS), IL-33 and HO-1. Conversely, a monocyte/

Abbreviations: ALT, alanine amino transferase; AST, aspartate amino transferase; CR, colorectal; CRLM, colorectal liver metastasis; DAMP, damage-associated molecular pattern; ELISA, enzyme-linked immunosorbent assay; GOT, glutamic oxaloacetic transaminase; GPT, glutamic pyruvic transaminase; HO-1, heme oxygenase-1; IL, interleukin; IR, ischemia-reperfusion; KC, Kupffer cells; MFI, median fluorescence intensity; RIPK3, receptor-interacting protein 3 kinase; TGF- β , transforming growth factor- β ; TNF- α , tumor necrosis factor- α ; WT mice, wild-type C57BL/6 mice.

Desislava Germanova and Jiri Keirsse contributed equally to the work.

macrophage-specific deficiency in HO-1 (HO-1^{flox/flox} LysM^{cre/wt}) or the blockade of HO-1 function led to the control of tumor progression post-liver IR. Importantly, host cell RIPK3 deficiency maintains the KC number upon IR, inhibits the IR-induced innate cell recruitment, increases the TNF level, decreases the HO-1 level and suppresses the tumor outgrowth. In conclusion, tumor recurrence in host undergoing liver IR is associated with the death of antitumoral KC and the recruitment of monocytes endowed with immunosuppressive properties. In both of which HO-1 inhibition would reinforce their antitumoral activity.

KEYWORDS

colorectal metastasis, inflammation, liver ischemia-reperfusion

1 | INTRODUCTION

Colorectal (CR) cancer is a frequent and often lethal tumor¹ with the development of liver metastases representing the main cause of mortality in patients.² Despite constant improvements in systemic and locoregional treatments, surgery remains the only potentially curative option yielding a disease-free survival superior to 10 years in 20% to 25% of the patients.³ Still, the majority of the patients operated for colorectal liver metastasis (CRLM) would relapse after curative-intent interventions, and a substantial proportion of them do so rapidly, suggesting a potential role for the operative stress in cancer progression. Indeed, several perioperative events related to surgery and anesthesia can directly influence the risk for cancer recurrence (reviewed in Reference 4). In particular, some degree of hepatic ischemia and subsequent ischemia-reperfusion (IR) injury are invariably imposed, related to the surgical procedure and to the vascular clamping maneuvers. In the clinical context, variable and eventually contradictory effects of hepatic IR injury on tumor growth were reported.⁵

Several pathways can contribute to the liver IR injury process. A prolonged ischemia causes a decrease in both adenosine triphosphate levels and pH with a calcium overload due to anaerobic metabolism. During the reperfusion phase, reactive oxygen and nitrogen species (ROS/RNS) generated through mitochondrial activity constitute the first wave of cytotoxic mediators that may directly target the hepatocyte viability. Hepatocyte death occurs through necrotic, necroptotic, apoptotic and autophagic mechanisms. Dying hepatocytes release cellular components named damage-associated molecular patterns (DAMPs) that may become immunostimulators when detected by innate immune cells like the dominant liver resident macrophages (ie, Kupffer cells [KC]) and dendritic cells. These cells translate these alarm signals into chemokine and cytokine secretion that could attract non-resident leukocytes, which are the source of the second wave of ROS/RNS, resulting in more severe tissue damage. However, how the multiple pathways of IR-induced liver injury evidenced so far impact the progression of CR cancer metastasis remains not fully understood.

A deeper understanding of the mechanisms of immunogenic and nonimmunogenic cell death shed new light on the potential impact of IR-induced cell damage within the tumor microenvironment.⁶ More

What's New?

Liver ischemia/reperfusion during surgical procedures such as partial hepatectomy contributes to colorectal liver metastasis progression. The underlying mechanisms are only partially understood. Here, using a mouse model of colorectal liver metastasis, the authors reveal that metastasis progression is correlated with the local production of TNF and HO-1 by resident Kupffer cells and recruited monocytes. Liver ischemia/reperfusion leads to a decrease in Kupffer cells, most likely through inflammatory cell death induction, that favours the recruitment of TNF-producing protective monocytes. The findings further suggest that monocyte activity could be reinforced to limit tumour progression through HO-1 inhibition.

particularly, receptor-interacting protein 3 kinase (RIPK3)-dependent cell death was revealed as a DAMP-related immunogenic type of cell death that could be induced upon liver IR⁷ and hereby influence anti-tumor immunity. This type of cell death can be engaged by death receptors (eg, tumor necrosis factor [TNF] receptor-1, CD95, TRAILR1 and TRAILR2) with a signaling pathway that depends on the oligomerization of RIPK1 and RIPK3 and the subsequent recruitment of Mixed lineage kinase domain like pseudokinase (MLKL) that translocates to the plasma membrane to induce its permeabilization.⁸ A dual role of RIPK3-dependent signaling in anticancer immunity was reported. Indeed, it may induce death of cancer cells that escaped apoptosis, but it might as well provide a cell death-independent tumor-promoting inflammatory microenvironment.^{9,10} The involvement of RIPK3-dependent cell death in IR-induced metastasis formation remains, however, an outstanding question.

In addition, it is not exactly understood which inflammatory components may affect tumor progression after liver IR. On one hand, the postsurgical acute phase response is associated with increased secretion of pro-inflammatory cytokines such as interleukin (IL)-1 β , IL-6,

and TNF that could favor antitumor cytotoxicity, although TNF was also reported as an accelerator of tumor cell proliferation.^{11,12} On the other hand, the concomitant release of anti-inflammatory mediators, including transforming growth factor (TGF)- β , IL-10, IL-1 receptor antagonist, IL-33 and iNOS may induce systemic immunosuppression. Finally, one of the major cytoprotective mechanisms activated upon liver ischemia is the induction of heme oxygenase-1 (HO-1), a heat-shock protein family member which catalyzes the breakdown of heme into biliverdin, carbon monoxide and free iron. Its action on cancer progression during liver IR was not yet demonstrated.

We bring new evidence on the impact of liver IR on local inflammation that contributes to the CRLM progression. We defined the local myeloid source of TNF and HO-1 during liver IR and identified their respective antagonist role in the tumor progression. We also analyzed the KC death pathway occurring upon liver IR in link with the metastatic development.

2 | MATERIALS AND METHODS

2.1 | Mice

Male C57BL/6 mice of 8 to 12 weeks old were used (Envigo, Zeist, The Netherlands). C57BL/6 $Hmox1^{LoxP}$ mice were obtained through the RIKEN BioResource Center (B6J.129P2- $Hmox1^{tm1Mym}$). Myeloid TNF KO mice (TNF^{M-KO} mice; TNF^{flox/flox}LysM^{Cre/wt} mice)¹³ and Myeloid HO-1 KO mice (HO-1^{M-KO} mice; $Hmox1^{flox/flox}$ LysM^{Cre/wt} mice) were mated at the Institute for Medical Immunology. RIPK3-KO mice were kindly provided by Peter Vandenabeele (Inflammation Research Center, VIB, Ghent, Belgium). CCR2-KO mice were purchased from The Jackson Laboratory (Bar Harbor, Maine).

2.2 | Cancer cell lines

All experiments were performed with confirmed mycoplasma-free cell lines using the MycoAlert Mycoplasma Detection Kit (Lonza Research Products, Basel, Switzerland). the RAW 264.7 cell line (RRID: CVCL_0493) was from ATCC (#TIB-71) and was grown in Roswell Park memorial institute (RPMI) 1640 medium supplemented with 10% heat-inactivated fetal bovine serum, 2 mM L-glutamine, 1 mM nonessential amino acids, 100 mM sodium pyruvate, penicillin (10 U/mL)-streptomycin (10 μ g/mL) and 10^{-5} M 2-ME (Lonza Research Products) at 37°C and 5% CO₂. The murine colon adenocarcinoma cell lines, MC-38 (RRID:CVCL_B288) and MC-32A, also called MC-38-CEA-2 (RRID:CVCL_5137), were obtained from Benoit Van den Eynde (UCL, Brussels, Belgium). The luciferase-expressing MC-38 was obtained from CIMA, Pamplona, Spain (MC-38^{luc}, RRID:CVCL_0A67).¹⁴ MC-38, MC-32A, and MC38^{Luc1} cell lines have recently been authenticated using short tandem repeat profiling by American Type Culture Collection (ATCC) (June 2020), and were all maintained in Dulbecco's Modified Eagle medium (DMEM) supplemented with the same reagents and 400 μ g/mL G418 (Geneticin, Invitrogen, Carlsbad, CA, USA).

2.3 | Experimental hepatic metastasis model

Under isoflurane inhalation anesthesia, a small midline laparotomy was performed on prehydrated (0.9% NaCl, 250 μ L) mice. Body temperature was maintained at 36.5°C to 37°C during the entire experiment. 10⁶ MC-38 cells were injected into the pulp of the anterior inferior pole of the spleen. After 10 minutes, splenectomy was performed to prevent massive tumor spread in the spleen. SHAM-operated mice underwent the same procedure with intrasplenic injection of 100 μ L of sterile PBS.

2.4 | Liver IR model

A partial hepatic ischemia was induced through the placement of an atraumatic vascular clamp across the three portal elements (hepatic arterial, portal vein and bile duct branch) of the left lateral lobe for 60 minutes, rendering approximately 30% of the liver ischemic. SHAM-operated splenectomized mice underwent the same procedure except for the clamping. Blood samples were taken through the tail vein at several time points postreperfusion (<50 μ L/time point). Liver glutamic pyruvic transaminase (GPT)/alanine aminotransferase (ALT) or glutamic oxaloacetic transaminase (GOT)/aspartate aminotransferase (AST) were measured in the serum with an auto analyzer (Modular P800, Hitachi, Mannheim, Germany). Using commercial kits (Boehringer, Mannheim, Germany), the measured rate of NADH oxidation at 340 nm is directly proportional to the catalytic activity of GPT or GOT.

2.5 | In vivo inhibitor treatment

Zinc protoporphyrin-9 (ZnPPIX, Frontier Scientific, Logan, Utah), a competitive inhibitor of the HO-1 was dissolved in 0,25 N NaOH. The pH 7.4 was achieved with 1 M HCl and further diluted with PBS. ZnPPIX was administered i.p. at 5 mg/kg on Days 1-3-5-7-9 post-liver IR.

2.6 | Histology

Formalin-fixed hepatic lobes of interest were embedded in paraffin. Liver sections of 5 μ m were stained with hematoxylin/eosin. Tumor load was evaluated by two independent anatomopathologists as a percentage of normal liver parenchyma replacement area. The Suzuki injury score was established as described.¹⁵

2.7 | Bioluminescence imaging

Before imaging, mice were shaved to decrease the light absorption and scattering of animal fur. Mice were anesthetized with 4% of isoflurane vaporized in 2 L/min O₂ and then maintained with 2% isoflurane in 0,3 L/min O₂ per mouse. Each animal received i.p. 150 mg/kg

body weight of D-luciferin (VivoGlo, Promega, Madison, WI, USA). Mice were immediately imaged in a Photon Imager RT (Biospace Lab, Nesles-la-Vallée, France) that dynamically counted the emitted photons for at least 30 minutes. Image analysis was performed with M3Vision (Biospace Lab) software. Regions of interest (ROIs) were drawn on mouse abdomen and then signal intensities were quantified individually for each mouse for intervals of 5 minutes corresponding to the maximum signal intensity plateau.

2.8 | Western blot analysis

Cell lines or liver homogenates were lysed in RIPA buffer containing protease inhibitors (Sigma-Aldrich, St. Louis, MI, USA). Protein analysis was performed as described.¹⁶ Primary antibodies used for western blot were RIPK3 pAb (Novus Biologicals, Centennial, CO, USA), caspase-3 mAb (Alexis Biochemicals, New York, NY, USA), cleaved caspase-3 mAb (Cell Signaling, Beverly, MA, USA) and Actin pAb (Sigma-Aldrich). Secondary antibodies used were donkey anti-rabbit IgG-Horseradish peroxidase (HRP) and sheep anti-mouse Ig-HRP were from GE Healthcare (Little Chalfont, England, UK).

2.9 | Enzyme-linked immunosorbent assay

Quantification of CCL2 in the serum and the liver homogenate was performed using enzyme-linked immunosorbent assay (ELISA) Duoset Kit according to manufacturer's instructions (R&D Systems, Minneapolis, Minnesota).

2.10 | Flow cytometry

The ischemic liver lobes were collected, weighted, and transferred into GentleMACS tubes (Miltenyi Biotec, Leiden, The Netherlands) supplemented with RPMI 1640 medium and collagenase A (Type III, Worthington Biochemicals, Lakewood, New Jersey) and DNase I (Roche) for two rounds of the m_liver_01 protocol of the gentleMACS dissociator (Miltenyi Biotec). After 20 minutes at 37°C, tubes completed the m_liver_02 protocol of the same dissociator. The obtained suspension was diluted in Fluorescence activated cell sorter (FACS) buffer and passed through a sterile 100 µm filter, centrifuged (440G, 5 minutes at 4°C) and resuspended for 3 minutes in ammonium-chloride-potassium lysis buffer. Cells were resuspended at a concentration of 10⁷ cells ml⁻¹ at 4°C and were incubated with FcγR-blocking antibodies, rat anti-mouse CD16/CD32 (2.4G2, RatlgG2b, BD Bioscience, Erembodegem, Belgium). Subsequently, each sample was incubated in the dark at 4°C for 20 minutes with a specific combination of fluorescently labeled antibodies (see Table S1). For intracellular staining, 10⁶ cells ml⁻¹ were incubated with Brefeldin A (eBioscience, San Diego, California) for 4 hours at 37°C prior to staining of extracellular markers. Cells were subsequently fixed using fixation buffer (eBioscience) for 20 minutes at room temperature. Permeabilization

buffer (eBioscience) was added and samples were centrifuged (440 g, 5 minutes at 4°C). Cells were then incubated with fluorochrome-labeled antibodies for 20 minutes and washed. Caspase-8 and caspase-1 activity assays were performed following manufacturer protocol. Cells were incubated with FAM-FLICA (Bio-Rad AbD, Hercules, CA, USA) an irreversible inhibitor of the caspase enzyme and dimethyl sulfoxide (Sigma Aldrich) for 1 hour before proceeding to standard extracellular staining. Samples were measured using the FACS Cantoll (BD Bioscience) and sorted using the FACS Ariall (BD Bioscience). Obtained data were analyzed using the FlowJo V9.3.2 software (FlowJo, Ashland, Oregon). The cell survival assay was performed as described.¹⁶

2.11 | RNA purification and real-time RT-PCR

RNA was extracted from ischemic liver lobes using an EZNA HP Total RNA Kit (Omega Bio-Tek, Norcross, Georgia). Reverse transcription (RT) and real-time polymerase chain reaction (PCR) were performed using Light-Cycler Multiplex RNA Virus Master (one-step procedure) on a Light-Cycler 480 apparatus (Roche Diagnostics, Mannheim, Germany) (see Table S2). Relative gene expression was established compared to the group of tumor inoculated C57BL/6 mice. The sequences of primers and probes are available on request.

2.12 | Statistics

Data were expressed as mean ± SEM. Unless specified, the significance was determined by analysis of variance using the one-way analysis of variance (ANOVA) test with the GraphPad Prism 6.0 software. A *P* value <.05 was considered statistically significant.

3 | RESULTS

3.1 | Liver IR induces injury and promotes the progression of colon carcinoma metastases

To mimic the impact of the surgical procedure used in the clinic to remove hepatic metastases, we used a preclinical model of warm hepatic IR in mice bearing liver metastases. Hereto, C57BL/6 mice were subjected to a 60-min portal pedicle clamping of the left hepatic lobe 2 days after liver implantation of colon carcinoma MC-38 cells through splenic inoculation (Figure S1A). First, we confirmed the IR-induced liver injury in metastasis-bearing mice by measuring increased serum ALT and AST levels and larger hepatocellular lesions reflected by an elevated Suzuki Injury score in MC-38 bearing mice after liver IR (T + IR) compared to SHAM-operated tumor-inoculated (T) mice (Figure S1B-D). We evaluated by histology the impact of liver IR on MC-38 metastatic growth. Ten days post-IR, the fraction of normal liver parenchyma replacement by tumor cells was higher in the left lobe of T + IR mice compared to T mice (Figure 1A). The same

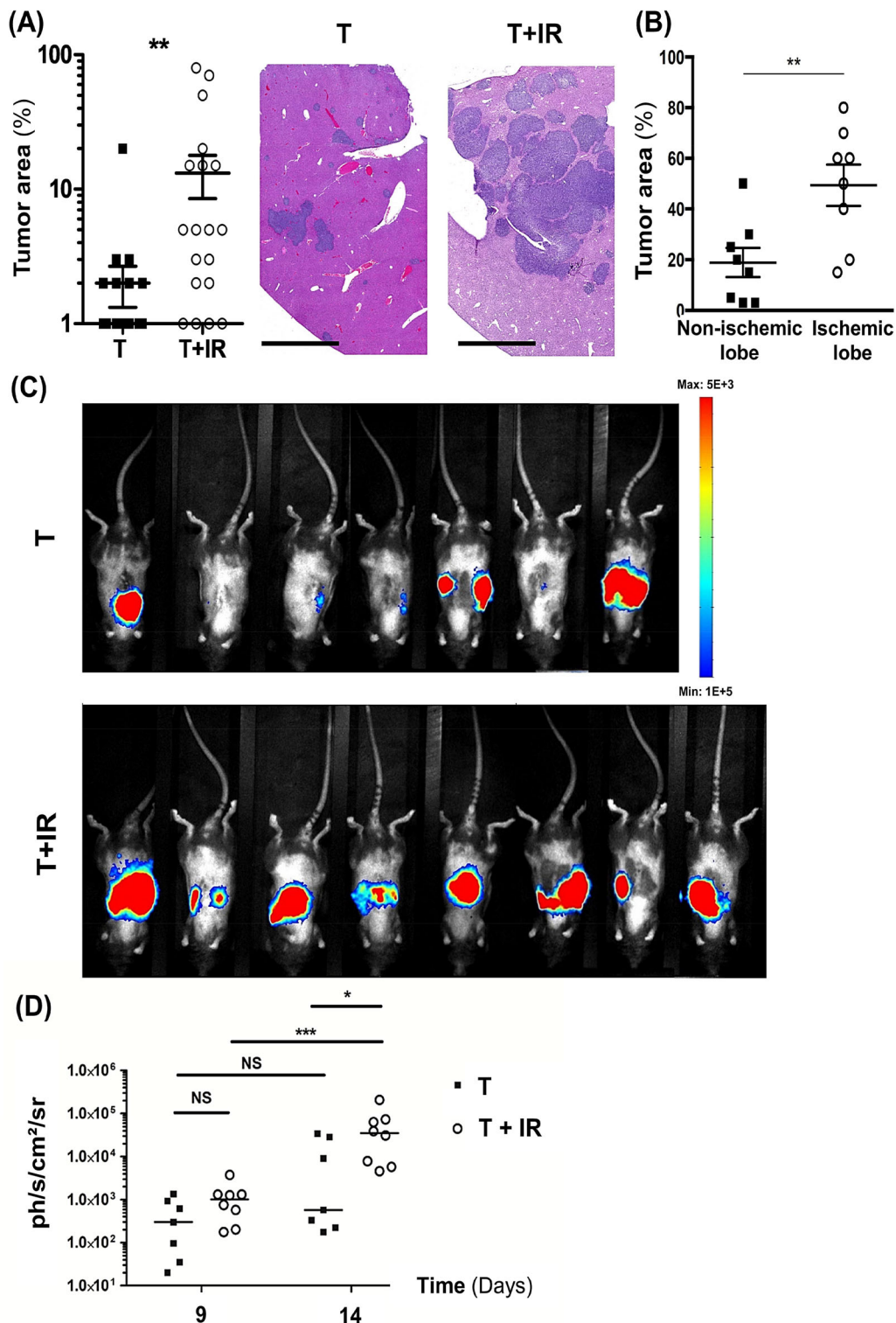


FIGURE 1 Liver IR-induces MC-38 outgrowth. A, (Left panel) Histological measurement of the percentage of MC-38 area in the liver of T and T + IR groups of C57BL/6 mice, 10 days posttumor inoculation (n = 25/group) (**P < .01, two-tailed nonparametric Mann-Whitney test). A, (Right panel) Representative images of histological observations. Scale bar, 1 mm. B, Histological measurement of the percentage of MC-38 area in ischemic vs nonischemic lobes in individual T + IR C57BL/6 mice (n = 8/group; **P < .01, two-tailed nonparametric Mann-Whitney test). C, Bioluminescence imaging. CCD camera image capture of C57BL/6 mice inoculated 14 days before with luciferase-MC-38 cells (T group) and undergoing liver IR 12 days before (T + IR group). D, Serial liver emitted photon quantification at 9 and 14 days postluciferase-MC-38 inoculation in C57BL/6 mice (*P < .05, and ***P < .001 two-tailed nonparametric Mann-Whitney test). IR, ischemia-reperfusion

observation was made by histological analysis using another colon carcinoma cell line MC-32-A in wild-type C57BL/6 mice (WT mice) (Figure S2). Moreover, in T + IR mice, the outgrowth of MC-38 cells was accelerated in the clamped liver lobe when compared to non-ischemic lobes of the same liver (Figure 1B). To allow noninvasive follow-up of tumor growth, luciferase-expressing MC-38 cells were administered in mice subsequently exposed or not to the IR protocol. As shown in Figure 1C,D, in T + IR mice, the abdominal light emission increased over time (from 9 to 14 days postinjection) and was higher 14 days after tumor inoculation compared to T mice.

3.2 | KC and monocytes are affected in metastases-bearing liver lobe upon IR

As stressed and dying hepatocytes are known sources of DAMPs, we assessed how IR impacts innate immune cells in the tumor-bearing liver lobe submitted to this stress. First, we observed that the number of KC (CD11b^{int}F4/80^{pos}Clec4E^{pos}Tim4^{pos}Ly6G^{neg} cells) was increased between 24 and 72 hours post-MC-38-inoculation in T mice, compared to SHAM-operated nontumor implanted (SHAM) mice, and that liver IR abrogated this KC expansion in T + IR mice (Figure 2A), suggesting an IR-induced KC death. We assessed the KC death pathway by monitoring the active caspase-8, active caspase-1 and specific RIPK3-dependent phosphorylation of MLKL (p-MLKL Ser345) for apoptosis, pyroptosis and necroptosis, respectively. While we could

not detect induction of caspase-8 or phosphorylation of MLKL, caspase-1 activity was significantly higher in KC 12 hours post-IR (Figure 2B). This suggests that the induction of pyroptosis is responsible for the decreased amount of KC observed upon IR.

Strikingly, nonresident leukocytes, neutrophils (CD11b^{hi} Ly6G^{hi} Ly6C^{int}) (Figure S3A) and classical monocytes (CD11b^{hi} Ly6G^{neg} Ly6C^{hi}), were prominently recruited within 60 hours posttumor inoculation (corresponding to 12 hours postreperfusion) and remained at increased levels 24 hours postreperfusion in the left liver lobe of T + IR mice compared to T mice or SHAM mice (Figure 2C). This early local inflammatory cell increase was accompanied by a chemokine/cytokine storm in the liver. CXCL-2, CXCL-10 and IL-6 gene transcripts, all potentially neutrophil chemoattractants and products, were more expressed in the IR-lobe from T + IR mice compared to the T mice (Figure S3B). CCL-2 protein, a monocyte chemoattractant, was also expressed at higher levels in the IR lobe and in the serum of T + IR mice (Figure 2D). We evaluated the impact of IR-induced monocyte influx on tumor growth by using CCL2 receptor-deficient mice (ie, CCR2) that exhibit defective monocytes recruitment during immune response. The MC-38 outgrowth induced upon liver IR was significantly higher in CCR2-KO mice compared to WT mice suggesting at least a partial protective role of monocytes (Figure 2E).

These data demonstrate that the surgical stress induced in a liver lobe with metastases induced KC pyroptosis and recruitment of neutrophils and monocytes. The latter could contribute partially to the control of the tumor growth.

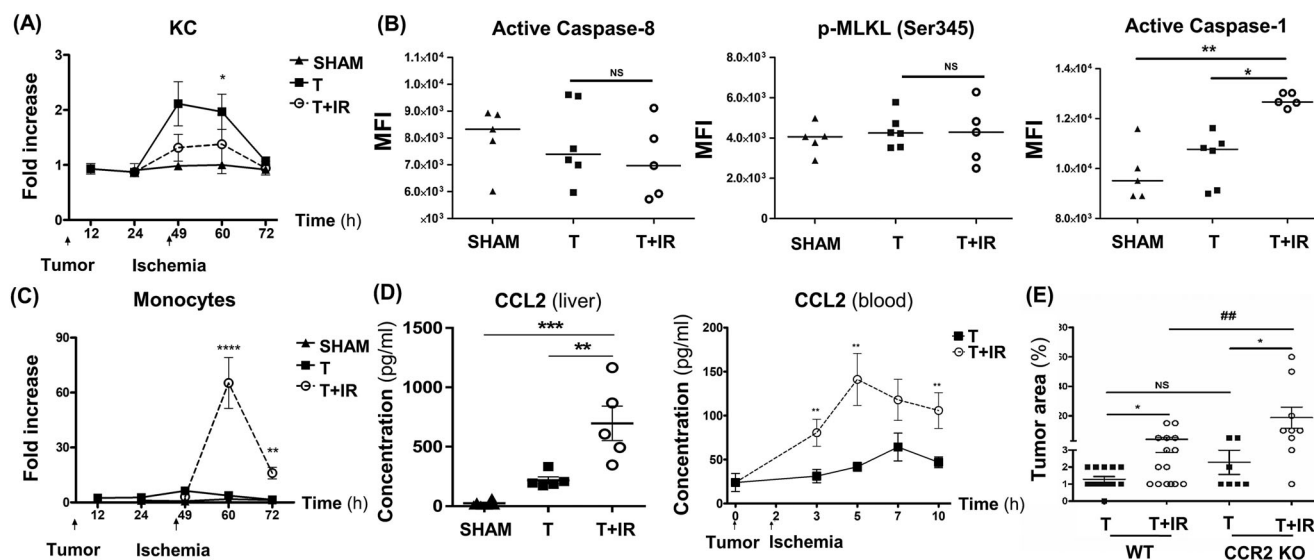


FIGURE 2 KC are impeded and monocytes recruited upon liver IR. A, Fold increase in number of KC g^{-1} of left liver lobe in SHAM, T and T + IR groups ($n = 5-20/$ group) of C57BL/6 mice over time ($*P < .05$ comparing T and T + IR groups with two-tailed nonparametric Mann-Whitney test). B, Median fluorescence intensity (MFI) of C57BL/6 KCs stained with fluorescent-labeled inhibitor of caspase-8 (left panel), Ser345 phosphorylated MLKL (p-MLKL Ser345/central panel) and fluorescent-labeled inhibitor of caspase-1 (right panel) 12 hours post-IR ($n = 5/$ group $*P < .05$, $**P < .01$, Kruskal-Wallis followed by Dunn's post hoc test). C, Fold increase in number of monocytes g^{-1} of left liver lobe in SHAM, T and T + IR group ($n = 5-20/$ group) of C57BL/6 over time ($**P < .01$, $****P < .0001$ comparing T and T + IR groups with a two-tailed nonparametric Mann-Whitney test). D, ELISA quantification of CCL2 protein levels from left liver lobe 2 hours post-IR (left panel) or blood (right panel) ($n = 6-10/$ group; $**P < .01$, $***P < .001$ two-tailed nonparametric Mann-Whitney test). E, Histological measurement of the percentage of MC-38 area in the liver of T and T + IR groups of C57BL/6 and CCR2 KO mice, 10 days post-tumor inoculation ($n = 7-15/$ group $* < .05$, $##P < .01$ Kruskal-Wallis followed by Dunn's post hoc test). ELISA, enzyme-linked immunosorbent assay; IR, ischemia-reperfusion; KC, Kupffer cells

3.3 | Monocytes that are recruited upon liver IR constitute a supplementary source of HO-1 and TNF

We noticed that compared to SHAM mice, T mice displayed a slight increase of liver TNF gene expression (Figure 3A) that could be interpreted by the increase of TNF-producing KC (Figure 3B). This TNF production could at least partially account for the control of tumor growth in T mice. Interestingly, we observed that compared to T or SHAM mice, the liver lobe of T + IR mice displayed a significant increased TNF and HO-1 gene transcript levels, as reported mediators to be associated with the IR-induced sterile inflammation (Figure 3A). Intracellular staining on immune cells from the MC-38-bearing liver lobe revealed that both recruited monocytes and, to a lesser extent, KC co-dominantly contributed to TNF and HO-1 production in T + IR mice (Figure 3B). Looking at Figure 3B, we can see that IR exerts opposite effects on monocytes and KC. Indeed, it significantly increased the amount of TNF- and HO-1-producing monocytes and decreased the amount of TNF- and HO-1-producing KC. For KC, this observation can only be explained by the kinetics data presented in Figure 2A since IR did not affect the intrinsic ability of these cells to produce both cytokines (Figure S4). On the opposite, increased frequency of TNF- and HO-1-producing monocytes following IR can be

due to two phenomena, an increased frequency of monocytes and an increased intrinsic capacity of those cells to produce both cytokines (Figure S4). In conclusion, liver IR induces the recruitment of monocytes that constitute an extra source of HO-1 and TNF while it has no significant impact on cytokines production by KC.

3.4 | Host RIPK3 promotes metastatic growth in liver lobe submitted to IR

We further explored the role of TNF receptor interacting RIPK3 kinase in the tumor-promoting microenvironment induced upon liver IR. First, we observed a much higher expression of the RIPK3 kinase within the liver parenchyma 24 hours post-IR in T + IR mice compared to T mice and SHAM mice (Figure 4A). We also noticed that the expression of the kinase was slightly upregulated in T mice (Figure 4A). Interestingly, we observed that KC expansion induced by the tumor did not occur in T RIPK3 KO mice (Figure 4B) suggesting a RIPK3-dependent proliferation signal induced by the tumor in resident KC. In addition, the accumulation of monocytes was strongly reduced (Figure 4B) in T + IR RIPK3-KO mice compared to T + IR WT mice. Remarkably, despite the reduced influx of inflammatory cells, TNF

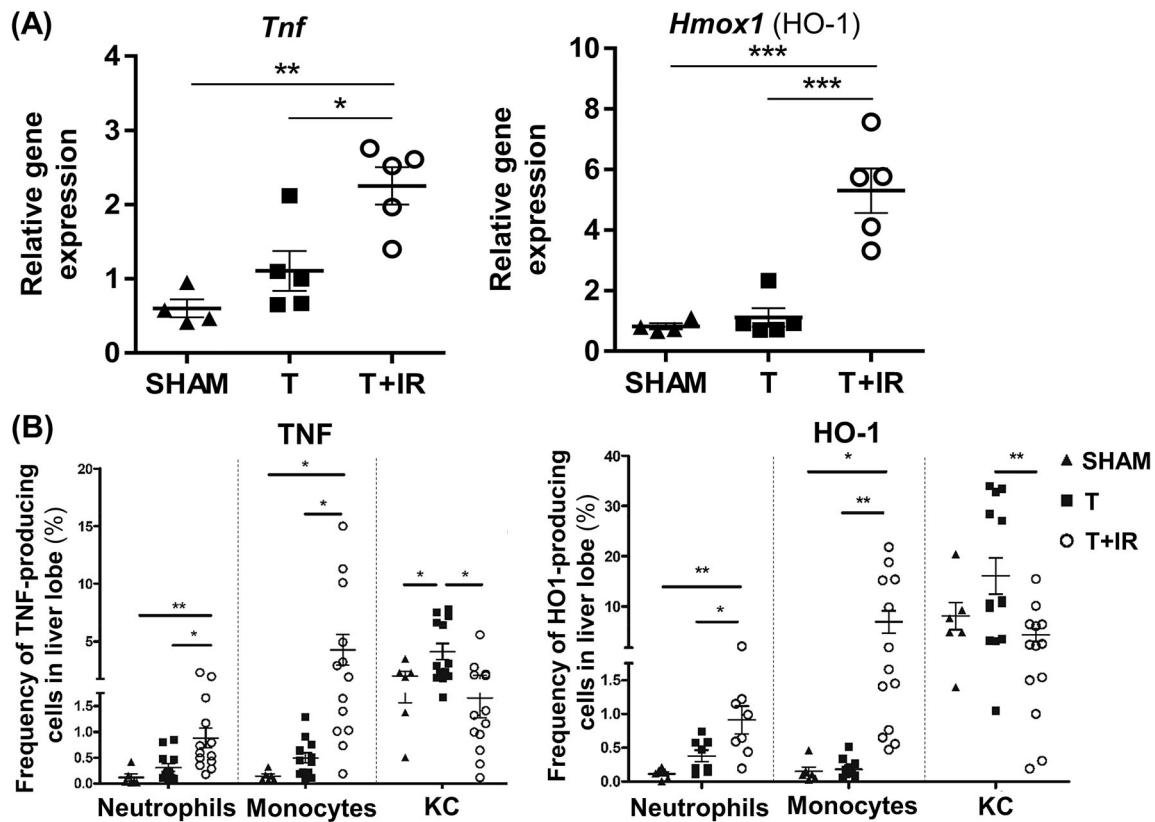


FIGURE 3 TNF and HO-1 are mainly produced by monocytes upon IR injury. A, TNF and HO-1 mRNA levels were measured from left liver lobe of SHAM, T and T + IR groups of C57BL/6 mice 2 hours post-IR. TNF and HO-1 expression were determined using Hypoxanthine Phosphoribosyltransferase (HPRT) as housekeeping gene and T group of mice to normalize (* $P < .05$, ** $P < .01$, *** $P < .001$ one-way ANOVA followed by Bonferroni's multiple comparison test). B, Frequency of indicated cell types producing TNF or HO-1 in the left liver lobe, 12 hours post-IR in SHAM, T and T + IR groups of C57BL/6 mice ($n = 413$ /group). Results were collected from three independent experiments (* $P < .05$, ** $P < .01$, Kruskal-Wallis followed by Dunn's post hoc test). HO-1, heme oxygenase-1; IR, ischemia-reperfusion; TNF, tumor necrosis factor

expression was even more induced in the affected liver lobe of T + IR RIPK3-KO mice compared to T + IR C57BL/6 mice (Figure 4C). Conversely, the induction of HO-1 was smaller in T + IR RIPK3 KO mice compared to T + IR C57BL/6 mice (Figure 4C). However, these changes were not reflected at the level of hepatocellular cell death, as demonstrated by an unaffected IR-induced hepatocellular death area in T + IR RIPK3-KO mice compared to T RIPK3-KO mice (Figure S1C-D). Finally, and most importantly, we observed that the IR-induced tumor progression was completely inhibited (Figure 4D) in T + IR RIPK3-KO mice compared to T + IR WT mice. This suggests that in RIPK3-KO mice, the surviving KC would be effective to limit the metastasis outgrowth through an increased synthesis of TNF and a decreased synthesis of HO-1 upon liver IR.

Together, these data suggest on one hand that hepatocellular RIPK3 activation induced upon tumor implantation contributes to resident KC expansion. On the other hand, RIPK3 upregulation induced upon liver IR contributes to myeloid-cell recruitment with a positive impact on liver HO-1 synthesis and a negative impact on liver TNF synthesis.

3.5 | TNF produced by myeloid cells upon liver IR is protective against metastasis outgrowth

We next focused on TNF, the major cytokine involved in the liver pathogenesis upon IR injury. We first aimed to evaluate the link

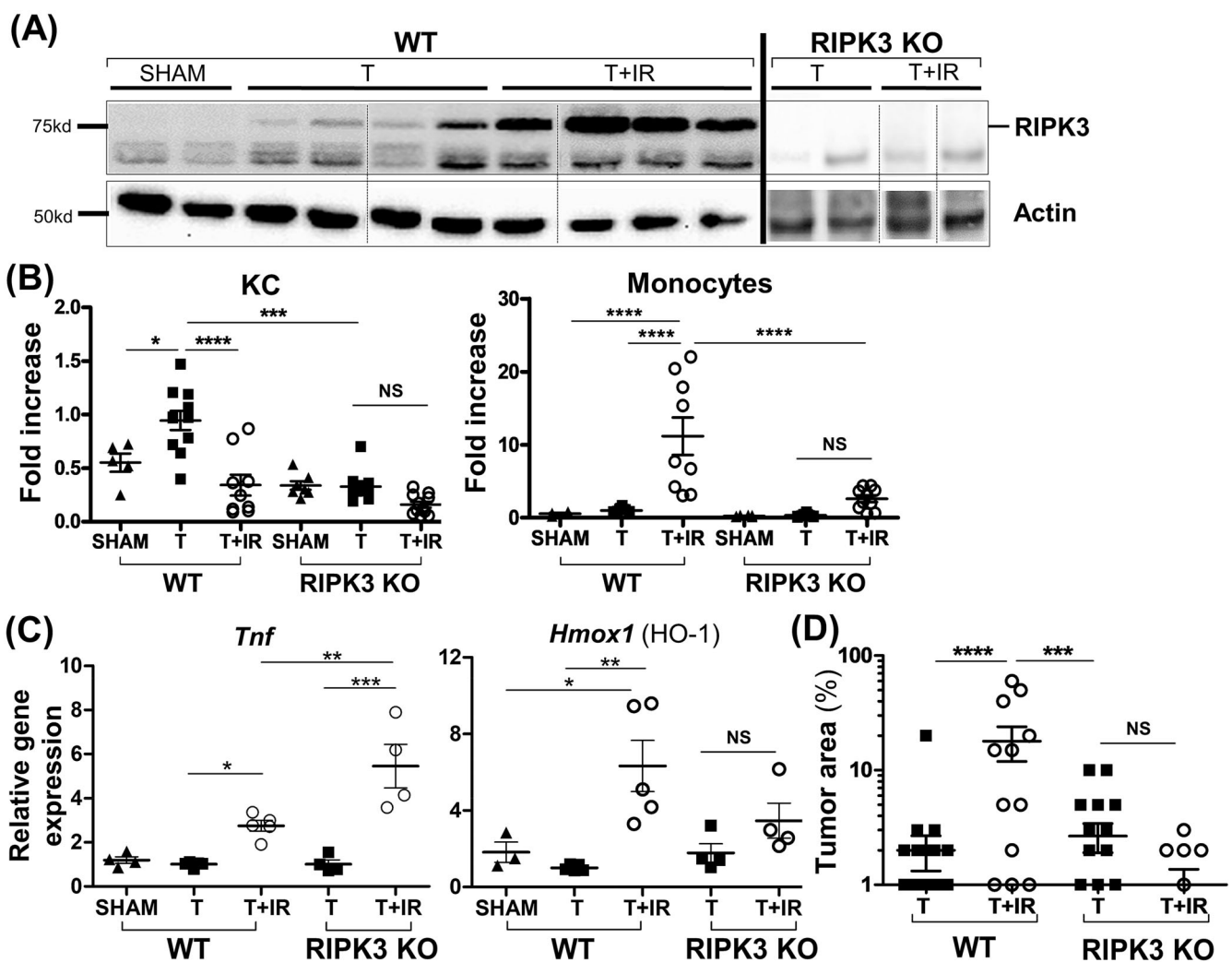


FIGURE 4 RIPK3-KO mice display resistance to IR induced MC38 cells outgrowth linked with a modification of TNF/HO-1 production. A, Representative western blot analysis of RIP3K and actin expressions in SHAM, T and T + IR groups of C57BL/6 or RIPK3^{-/-} mice 24 hours post-IR. B, Fold increase in number of KC g⁻¹ and monocytes g⁻¹ of left liver lobe in SHAM, T and T + IR groups (n = 5-10/group) of C57BL/6 and RIPK3-KO mice 12 hours post-IR. Mice were normalized to the T group of C57BL/6 strain. C, TNF and HO-1 mRNA levels were measured 2 hours post-IR using HPRT as housekeeping gene and T group of RIPK3-KO mice to normalize. D, Histological measurement of the percentage of tumor replacement area in the liver of T and T + IR groups of C57BL/6 and RIPK3-KO mice 10 days posttumor inoculation (n = 10-12/group; ***P < .001 and ****P < .0001, one-way ANOVA followed by Bonferroni's multiple comparison test). HO-1, heme oxygenase-1; IR, ischemia-reperfusion; RIPK3, receptor-interacting protein 3 kinase; TNF, tumor necrosis factor

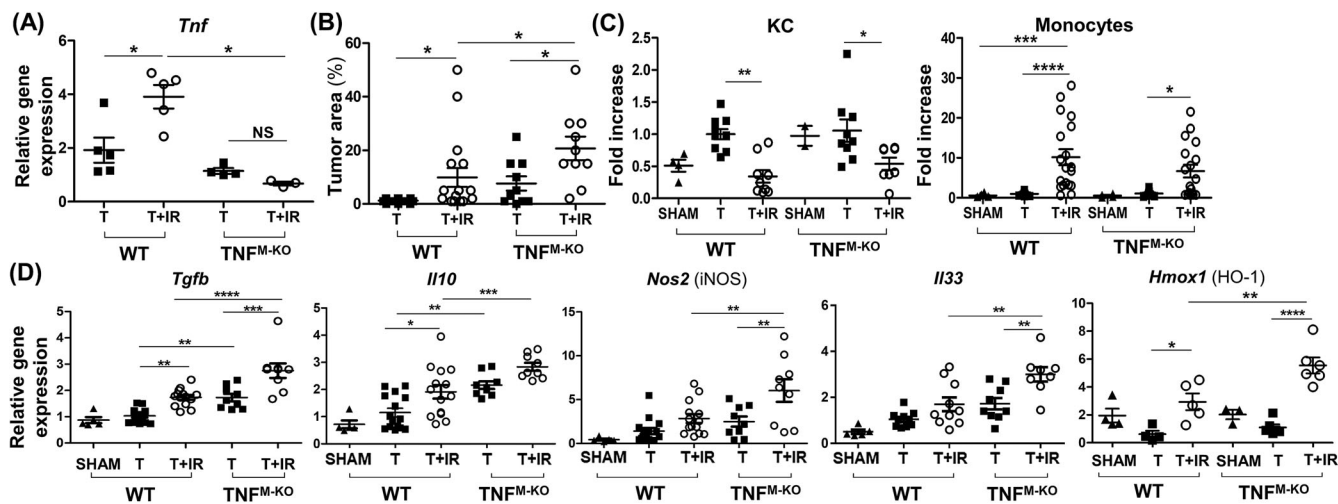


FIGURE 5 TNF inhibits MC38 cells outgrowth by limiting expression of anti-inflammatory factors upon IR. A, Left liver lobe from groups of C57BL/6 and TNF^{M-KO} mice were collected 8 days post-IR for TNF transcript measurement using HPRT as housekeeping gene and T group of C57BL/6 mice to normalize ($n = 3-5$ /group). B, Histological measurement of the percentage of tumor area in the liver of T and T + IR groups of C57BL/6 and $TNF-1^{M-KO}$ mice 10 days posttumor inoculation ($n = 9-13$ /group). C, Fold increase in number of KC g^{-1} and monocytes g^{-1} of left liver lobe in SHAM, T and T + IR groups ($n = 3-17$ /group) of C57BL/6 and TNF^{M-KO} mice 12 hours post IR. Mice were normalized to the T group of C57BL/6 strain. D, Left liver lobe from groups of C57BL/6 and TNF^{M-KO} mice were collected 8 days post-IR for indicated transcript measurement using HPRT as housekeeping gene and T group of C57BL/6 mice to normalize ($n = 5-13$ /group). (* $P < .05$, ** $P < .01$, *** $P < .001$, **** $P < .0001$ one-way ANOVA followed by Bonferroni's multiple comparison test). HO-1, heme oxygenase-1; IR, ischemia-reperfusion; TNF, tumor necrosis factor

between TNF and IR-induced hepatic metastasis outgrowth. Since monocytes and KC are the major producers of TNF in our model, we performed the liver IR stress on MC-38-inoculated TNF^{M-KO} mice, in which both cell-types are TNF-defective. First we confirmed that TNF transcripts were not induced in the ischemic liver lobe of these KO mice compared to WT mice (Figure 5A). Interestingly TNF deficiency in these cells was associated with an increase in MC-38 metastasis (Figure 5B) and a decrease in hepatocellular injury (Figure S1C,D) as compared to WT mice, illustrating that monocyte/KC-derived TNF has a protective role both in T and T + IR mice. Of note, the IR-induced defect of KC accumulation and the increase in liver monocyte numbers (Figure 5C) were similar in TNF^{M-KO} mice and WT mice. Together, these data demonstrate that the monocyte/KC source of TNF contributes to hepatocellular injury, but at the same time provides protection against liver metastasis in tumor-bearing mice undergoing IR stress.

One of the antimetastatic mechanisms of TNF could be a direct cytotoxic effect of this cytokine on MC-38 cells. Indeed, an active caspase-3-dependent and RIPK3-independent type of cell death, suggestive of apoptosis, was induced by recombinant TNF in MC-38 cancer cells (Figure S5A-C).

3.6 | HO-1 produced by myeloid cells upon liver IR stimulates metastasis outgrowth

HO-1, known to dampen inflammatory responses as opposed to TNF, was upregulated mainly in KC and monocytes upon IR (Figure 3B). This was accompanied by the upregulation of several

anti-inflammatory mediator transcripts, including TGF- β and IL-10 in IR-stressed T + IR mice compared to nonstressed T mice (Figure 5D) suggesting that an anti-inflammatory/immunosuppressive milieu is contributing to metastasis outgrowth in ischemic mice. In line with this hypothesis, the increased metastasis progression in T + IR TNF^{M-KO} mice was associated with a significantly higher level of TGF- β , IL-10, iNOS and IL-33 liver transcripts compared to T + IR WT mice (Figure 5D). Similar to WT mice, TNF^{M-KO} monocytes kept their ability to synthesize HO-1 upon liver IR (40% of all monocytes are HO-1 positive), but HO-1 expression is even increased in TNF^{M-KO} KC (80% of all KC are HO-1 positive in TNF^{M-KO} (Figure 6A). These observations encouraged us to further evaluate the impact of HO-1 on IR-induced tumor progression. Using $HO-1^{M-KO}$ mice in which myeloid cells are defective in HO-1, we observed that the increased MC-38 liver metastasis progression in T + IR mice was abrogated (Figure 6B) and was correlated with the IR-induced recruitment of monocytes and decrease in KC (Figure 6C). Finally, treatment with ZnPPiX, a competitive inhibitor of HO-1, also prevented the enhanced metastasis progression in T + IR WT mice (Figure 6D). These data demonstrate that HO-1 induction in myeloid cells by liver IR contributes to metastasis outgrowth and that a blockade of this mediator may have therapeutic potential.

4 | DISCUSSION

Liver resections performed for colorectal cancer (CRC) metastases systematically initiate IR perioperative acute phase response. The

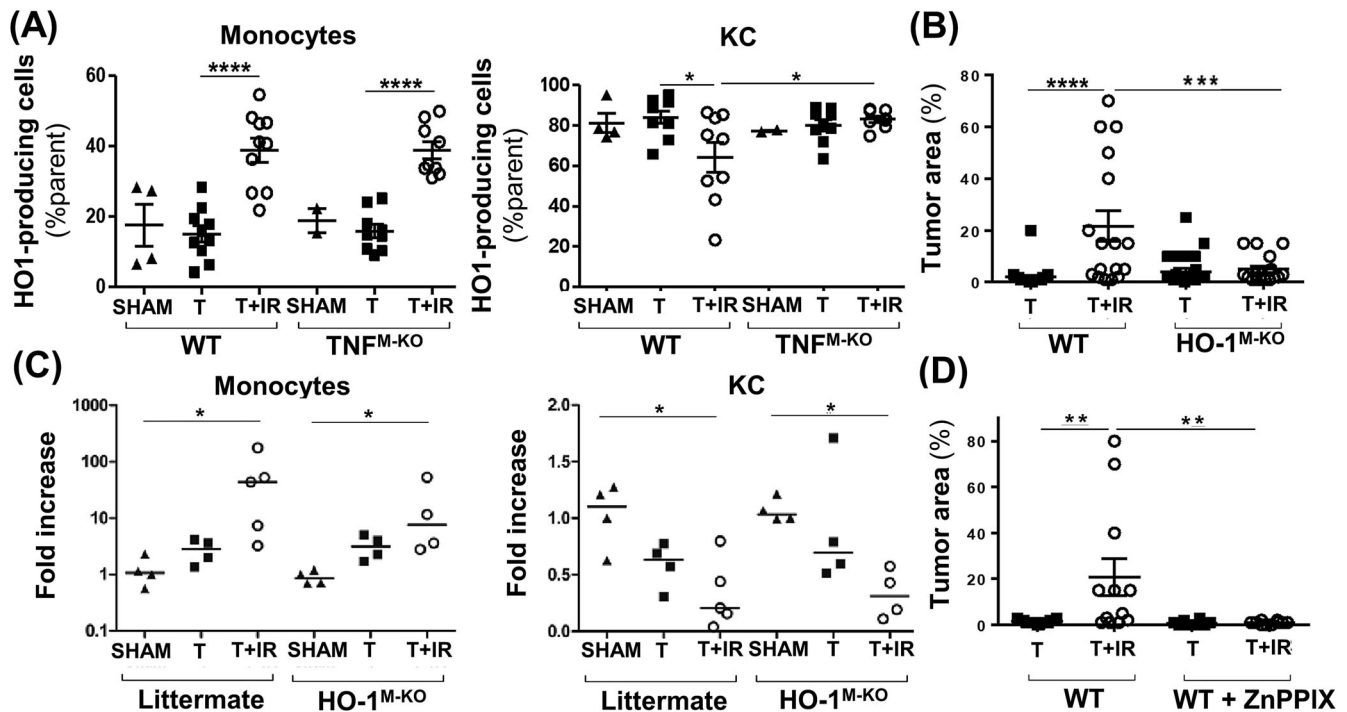


FIGURE 6 HO-1 participates in IR-induced MC38 cells outgrowth without modifying the kinetics of monocytes and KC. A, Frequency of monocytes and KC producing HO-1 in the left liver lobe, 12 hours post-IR in SHAM, T and T + IR groups of C57BL/6 or TNF^{M-KO} mice (n = 3-17/group). Results were collected from 3 independent experiments (**P* < .05, *****P* < .0001, one-way ANOVA followed by Bonferroni's multiple comparison test). B, Histological measurement of the percentage of tumor area in the liver of T and T + IR groups of C57BL/6 and HO-1^{M-KO} mice 10 days post tumor inoculation (n = 8-16/group) (***P* < .001, *****P* < .0001, one-way ANOVA followed by Bonferroni's multiple comparison test). C, Fold increase in number of KC g⁻¹ and monocytes g⁻¹ of left liver lobe in SHAM, T and T + IR groups (n = 4-5/group) of HO-1^{M-KO} mice and littermates 12 hours post-IR. Mice were normalized to the SHAM group of each strain (**P* < .05, Kruskal-Wallis followed by Dunn's post hoc test). D, Histological measurement of the percentage of tumor area in the liver of T and T + IR groups of ZnPIX-treated C57BL/6 mice 10 days posttumor inoculation. (***P* < .01, one-way ANOVA followed by Bonferroni's multiple comparison test). HO-1, heme oxygenase-1; IR, ischemia-reperfusion; KC, Kupffer cells; TNF, tumor necrosis factor

associated tissue damaging effects may have a significant impact on postoperative organ functions and on preexisting ignored hepatic micrometastases. This could happen during two-step liver resection or when hepatectomy is preceded by portal vein embolization or by intraarterial treatment. Indeed, several reports from rodent and clinical studies^{4,17} described accelerated outgrowth of residual tumors following surgical stress and direct tissue trauma that could be mimicked by the placement of a vascular clamp across the portal vein, hepatic artery and bile duct branch to one liver lobe. Understanding the effects of surgical stress and IR on tumor growth is thus essential to develop new perioperative therapeutic strategies aiming at reducing the risk of cancer recurrence. We bring new insights on the reported controversial effects of the inflammatory response initiated by liver surgical resection in patients.

KC are playing a role in arresting circulating tumor cells and controlling metastatic growth in the liver.¹⁸ Accordingly, they have an antitumoral effect in the early phase of CRLM implantation through, amongst others, IL-1 β , IL-6 and TNF.^{19,20} Several mechanisms can account for the antimetastatic activities of KC: cytotoxicity through protease or ROS-mediated lysis,^{19,21,22} CD95-mediated tumor cell apoptosis,²³ and collaboration with other effector cells, like

neutrophils, Natural Killer (NK) cells, NK T cells or T cells, through IL-12 or interferon (IFN)- γ release.²⁴ Like other reports,²⁵ we observed a significantly increased number of KC in the early stages of MC-38 CRLM implantation. We also showed that the tumor-induced KC accumulation was abrogated in RIPK3-KO mice suggesting a RIPK3-dependent signaling with a proliferation message or survival message to KC.²⁶ Our data showed that in WT mice, the tumor-induced KC expansion is inhibited upon liver IR, which correlates with a higher tumor progression.

We concluded that liver IR led to the activation of caspase-1 in KC, inducing their death via pyroptosis, a phenomenon that would be abrogated in RIPK3-KO mice. The mechanisms of how RIPK3 could induce the activation of caspase-1 remain to be determined. Usually, caspase-1 is activated through the formation of the NLRP3 inflammasome. This leads to the maturation of IL-1 β but can also induce cell death via the cleavage of gasdermin D and subsequent induction of pyroptosis.²⁷ Previous reports have shown that RIPK3 was able to activate NLRP3 independently of MLKL presence in bone marrow-derived macrophages.²⁸ Moreover, in dendritic cells, RIPK3-dependent activation of NLRP3 (and therefore activation of caspase-1) is regulated by caspase-8 activity.²⁹ Our results hint

toward the existence of a similar mechanism occurring in KC following IR since we could detect an IR-dependent activation of caspase-1 (and not caspase-8) in these cells.

Other mechanisms may explain how liver IR favors metastases outgrowth. Neutrophils were previously highlighted as first-line responders after surgical stress that may promote the development and progression of liver metastases.³⁰ Their recruitment to the premetastatic site was shown to be crucial to allow lung metastases to proliferate through their formation of extracellular traps for circulating cells.³¹ We monitored their presence in the early events post liver IR and their role in the liver IR-induced tumor outgrowth should be explored.

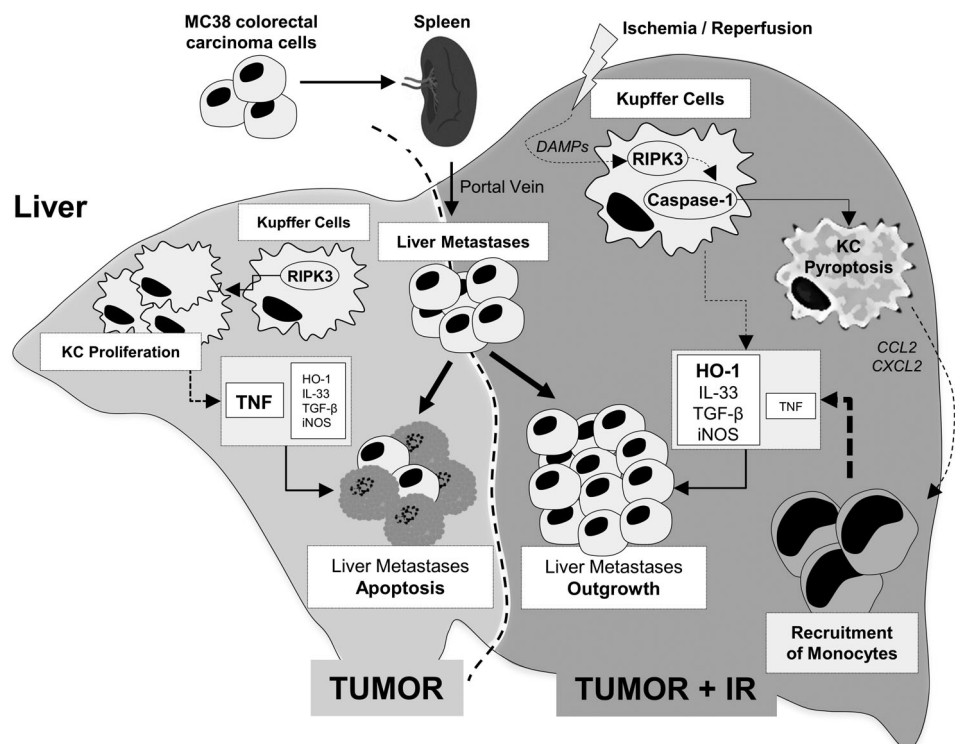
During the initial response to liver IR, we showed that CCL2 was produced at high levels, probably by KC, but also by tumor cells, since MC-38 secretes CCL2 (not shown). As a consequence, Ly-6C^{high} blood monocytes rapidly infiltrate the tissue to massively contribute to the macrophage pool. CCL2 was described as critical to potentially generate myeloid-derived suppressor cells that allow tumor evasion.³² Moreover, infiltrating monocytes can exert an anti- or pro-inflammatory action during liver ischemia that sustains tissue inflammation and damage. Here we demonstrate that they became an additional source of TNF and HO-1 that overall lead to tumor outgrowth. Along the same line, compared to T + IR C57BL/6 mice, an increased induction of TNF and a lower induction of HO-1 are observed in T + IR RIPK3-KO mice, which is correlated with inhibition of tissue injury, monocyte recruitment and tumor outgrowth.

How the local production of TNF may impact the IR-induced tissue damage and the growth of tumor cells was extensively studied with opposite outcomes. Concerning IR injury, TNF is considered as

one of the key molecules mediating the tissue injury. It acts primarily through its interaction with TNFR1 that could initiate in hepatocytes both programmed death pathways, apoptosis and necroptosis.³³ But the TNF/TNFR1 interaction at the cell membrane also promotes hepatocyte survival and proliferation through NF- κ B and MAPK pathways, both of which are crucial for liver regeneration after tissue damage.³⁴ Concerning tumor progression, many evidences highlighted that depending on the tumor type, the stage of the tumor or its microenvironment, the TNF-mediated inflammatory response may also have opposite effects.³⁵ Accumulating evidence suggest that TNF signaling is definitely shaping the tumor microenvironment and paradoxically, many studies highlighted the tumor promoting properties of TNF. Increased expression of TNF in CR cancer specimen from patients was associated with advanced tumoral stages.^{36,37} Animal models of TNF overexpression in the tumor microenvironment promote cancer development and enhanced metastasis.³⁸ In another model, macrophage-derived inhibitor of nuclear factor kappa B kinase (IKK) β promoted CR cancer via the upregulation of TNF, uncovering the link between nuclear factor-kappa B (NF- κ B) activation, inflammation and cancer.³⁹ The local production of TNF that stimulates NF- κ B in hepatocytes triggers hepatocarcinogenesis⁴⁰ and interestingly, the role of TNF in cancer cachexia would be more related to tumor-derived TNF than host-derived TNF.⁴¹ Blocking TNF in the tumor microenvironment was even proposed as a therapeutic approach to arrest tumor metastases and prolong survival⁴² since the suppressive activity of human Treg is strongly dependent on TNF.⁴³

In contrast, the present study shows a protective role of TNF acutely produced locally by KC and by infiltrating monocytes upon

FIGURE 7 Summary figure. Liver metastases have been induced through the injection of MC-38 colorectal carcinoma cells in the spleen. In a nonischemic setting, liver metastases implantation provokes a RIPK3-dependent proliferation of KC. By their ability to produce TNF, KC induce the apoptosis of MC-38. Upon liver IR, KC undergo an inflammatory cell death (pyroptosis) that is mediated by RIPK3/caspase-1 signaling pathway and that triggers a CCL2-dependent monocytes recruitment. This allows the activation of a strong liver cytokine storm, dominated by immunosuppressive factors, such as HO-1, that favors metastases outgrowth. IR, ischemia-reperfusion; KC, Kupffer cells; RIPK3, receptor-interacting protein 3 kinase; TNF, tumor necrosis factor



liver IR. Therefore, our data support the concept that local production of TNF by myeloid cells during liver IR may facilitate liver metastases destruction by apoptosis in contrast to the effects of the increased systemic TNF levels that would favor pro-tumoral effects of this surgical procedure due to uncontrolled inflammatory damage.⁴⁴ A moderate LysM activity was also described in erythroid and lymphoid cells.⁴⁵ As we used LysM-cre mice, the potential impact of TNF and HO-1 inhibition in some lymphoid cells could be further explored in this model.

TNF can interact through TNFR1 and leads to the formation of either complex IIa/b or to the formation of the necrosome, a signaling complex that relies on RIPK1, RIPK3 and MLKL. RIPK3 is thus a potential downstream element of TNF signaling. The RIPK3/MLKL activation in macrophages induced by phagocytosis of bacteria was reported to enhance the production of CCL2 and IL-1 β .²⁶ This underlies the importance of RIPK3 in the regulation of inflammatory responses. On the other hand, HO-1 is an anti-inflammatory molecule that is produced in KC following TLR4 activation.⁴⁶ This TLR4-dependent production relies on TNF signaling. HO-1 expression is induced in our model since IR injury induces a massive release of DAMPs (which are potent TLR4 activator) and TNF. HO-1 cytoprotective effect against TNF-induced cell death makes it therefore a potent regulator of TNF functions. While there is actually no data reporting a direct effect between HO-1 and RIPK3, the balance of their respective activities seems crucial in determining cell death and inflammatory state of cells induced by TNF.

We further highlighted here the role of TNF to dampen suppressive pathways, such as the reported suppressive effect of TNF on HO-1 induction.⁴⁷ Indeed, KC and infiltrating monocytes are the main source of anti-inflammatory molecules including the antioxidant HO⁴⁸ that has a cytoprotective effect for hepatocyte viability during IR injury and that limits apoptosis and inflammation.⁴⁹ This oxidative defense mechanism that promotes tissue repair could favor tumor progression due to the indirect action of HO-1, expressed in regulatory T cells to down-modulate T cell-mediated immune responses.⁵⁰ Indeed, we demonstrated here that higher induction of HO-1 in infiltrating monocytes is observed upon IR, and that myeloid-expressed HO-1 promoted tumor outgrowth. Particularly interesting is the finding that an inhibition of HO-1 leads to protection against liver metastasis outgrowth. In conclusion (Figure 7), liver metastases implantation provokes a RIPK3-dependent proliferation of KC in which the TNF production is activated. In this nonischemic setting, KC have the ability to induce a TNF-dependent tumor apoptosis. Upon liver IR, KC undergo an inflammatory cell death (pyroptosis) that triggers a CCL2-dependent monocyte recruitment. This allows the activation of a strong liver cytokine storm that is dominated by immunosuppressive factors, such as HO-1 that favor metastases outgrowth.

ACKNOWLEDGMENTS

We thank Alain Beschin, David Torres and Frédéric Paulart for scientific expertise and Philippe Horlait, Laurent Depret, Christophe Notte, Grégory Waterlot and Samuel Vanderbiest for animal care. Our study was supported by the Télévie-Fonds National de la Recherche Scientifique (FNRS, Belgium), the Fonds Erasme, the Foundation

Against Cancer and the Fonds pour la recherche médicale dans le Hainaut (FRMH). The CMMI is supported by the European Regional Development Fund and the Walloon Region.

CONFLICT OF INTEREST

The authors declare no potential conflict of interest.

DATA AVAILABILITY STATEMENT

The data that support the findings of our study are available from the corresponding author upon reasonable request.

ETHICS STATEMENT

All animals were housed and bred in our specific pathogen-free animal facility and received humane care according to the criteria outlined in the "Guide for the Care and Use of Laboratory Animals" prepared by the National Academy of Sciences (NIH publication 86-23 revised 1985). The institutional Animal Care and Local Use Committee approved the animal study (protocol CEBEA-BUC-2013-06).

ORCID

Véronique Flamand  <https://orcid.org/0000-0002-8906-3758>

REFERENCES

- Douaier J, Ravipati A, Grams B, Chowdhury S, Alatisse O, Are C. Colorectal cancer—global burden, trends, and geographical variations. *J Surg Oncol*. 2017;115:619-630.
- Manfredi S, Lepage C, Hatem C, Coatmeur O, Faivre J, Bouvier AM. Epidemiology and management of liver metastases from colorectal cancer. *Ann Surg*. 2006;244:254-259.
- Adam R, Yi B, Innominato PF, et al. Resection of colorectal liver metastases after second-line chemotherapy: is it worthwhile? A LiverMetSurvey analysis of 6415 patients. *Eur J Cancer*. 2017;78:7-15.
- Hiller JG, Perry NJ, Pouligiannis G, Riedel B, Sloan EK. Perioperative events influence cancer recurrence risk after surgery. *Nat Rev Clin Oncol*. 2018;15:205-218.
- Yamashita S, Venkatesan AM, Mizuno T, et al. Remnant liver ischemia as a prognostic factor for cancer-specific survival after resection of colorectal liver metastases. *JAMA Surg*. 2017;152:e172986.
- Pitt JM, Kroemer G, Zitvogel L. Immunogenic and non-immunogenic cell death in the tumor microenvironment. *Advances in Experimental Medicine and Biology*. Switzerland: Springer Nature; 2017:65-79.
- Liu B, Qian J-M. Cytoprotective role of heme oxygenase-1 in liver ischemia reperfusion injury. *Int J Clin Exp Med*. 2015;8:19867-19873.
- Krysko O, Aaes TL, Kagan VE, et al. Necroptotic cell death in anti-cancer therapy. *Immunol Rev*. 2017;280:207-219.
- Hänggi K, Vasilikos L, Valls AF, et al. RIPK1/RIPK3 promotes vascular permeability to allow tumor cell extravasation independent of its necroptotic function. *Cell Death Dis*. 2017;8:e2588.
- Seifert L, Werba G, Tiwari S, et al. The necrosome promotes pancreatic oncogenesis via CXCL1 and Mincle-induced immune suppression. *Nature*. 2016;532:245-249.
- Balkwill F. Tumour necrosis factor and cancer. *Nat Rev Cancer*. 2009;9:361-371.
- Szlosarek P, Charles KA, Balkwill FR. Tumour necrosis factor- α as a tumour promoter. *Eur J Cancer*. 2006;42:745-750.
- Grivennikov SI, Tumanov AV, Liepinsh DJ, et al. Distinct and non-redundant in vivo functions of TNF produced by T cells and macrophages/neutrophils: protective and deleterious effects. *Immunity*. 2005;22:93-104.

14. Zabala M, Alzuguren P, Benavides C, et al. Evaluation of bioluminescent imaging for noninvasive monitoring of colorectal cancer progression in the liver and its response to immunogene therapy. *Mol Cancer*. 2009;8:2.
15. Loi P, Yuan Q, Torres D, et al. Interferon regulatory factor 3 deficiency leads to interleukin-17-mediated liver ischemia-reperfusion injury. *Hepatology*. 2013;57:351-361.
16. Preyat N, Rossi M, Kers J, et al. Intracellular nicotinamide adenine dinucleotide promotes TNF-induced necroptosis in a siruin-dependent manner. *Cell Death Differ*. 2016;23:29-40.
17. Van Der Bilt JDW, Kranenburg O, Nijkamp MW, et al. Ischemia/reperfusion accelerates the outgrowth of hepatic micrometastases in a highly standardized murine model. *Hepatology*. 2005;42:165-175.
18. Bayón LG, Izquierdo MA, Sirovich I, Van Rooijen N, Beelen RHJ, Meijer S. Role of Kupffer cells in arresting circulating tumor cells and controlling metastatic growth in the liver. *Hepatology*. 1996;23:1224-1231.
19. Matsumura H, Kondo T, Ogawa K, et al. Kupffer cells decrease metastasis of colon cancer cells to the liver in the early stage. *Int J Oncol*. 2014;45:2303-2310.
20. Minami S, Furui J, Kanematsu T. Role of carcinoembryonic antigen in the progression of colon cancer cells that express carbohydrate antigen. *Cancer Res*. 2001;61:2732-2735.
21. Wasserman AJ, Laskin DL. Differential sensitivity of tumor targets to liver macrophage-mediated cytotoxicity. *Cancer Res*. 1987;47:6686-6691.
22. Gardner CR, Wasserman AJ, Laskin DL. Liver macrophage-mediated cytotoxicity toward mastocytoma cells involves phagocytosis of tumor targets. *Hepatology*. 1991;14:318-324.
23. Song E, Chen J, Ouyang N, Wang M, Exton MS, Heemann U. Kupffer cells of cirrhotic rat livers sensitize colon cancer cells to Fas-mediated apoptosis. *Br J Cancer*. 2001;84:1265-1271.
24. Racanelli V, Rehmann B. The liver as an immunological organ. *Hepatology*. 2006;43:S54-S62.
25. Timmers M, Vekemans K, Vermijlen D, et al. Interactions between rat colon carcinoma cells and kupffer cells during the onset of hepatic metastasis. *Int J Cancer*. 2004;112:793-802.
26. Blériot C, Dupuis T, Jouvion G, Eberl G, Disson O, Lecuit M. Liver-resident macrophage Necroptosis orchestrates type 1 microbicidal inflammation and type-2-mediated tissue repair during bacterial infection. *Immunity*. 2015;42:145-158.
27. Shi J, Gao W, Shao F. Pyroptosis: gasdermin-mediated programmed necrotic cell death. *Trends Biochem Sci*. 2017;42:245-254.
28. Lawlor KE, Khan N, Mildenhall A, et al. RIPK3 promotes cell death and NLRP3 inflammasome activation in the absence of MLKL. *Nat Commun*. 2015;6:6282.
29. Kang TB, Yang SH, Toth B, Kovalenko A, Wallach D. Caspase-8 blocks kinase RIPK3-mediated activation of the NLRP3 inflammasome. *Immunity*. 2013;38:27-40.
30. Wculek SK, Malanchi I. Neutrophils support lung colonization of metastasis-initiating breast cancer cells. *Nature*. 2015;528:413-417.
31. Tohme S, Yazdani HO, Al-Khafaji AB, et al. Neutrophil extracellular traps promote the development and progression of liver metastases after surgical stress. *Cancer Res*. 2016;76(6):1367-1380.
32. Kudo-Saito C, Shirako H, Ohike M, Tsukamoto N, Kawakami Y. CCL2 is critical for immunosuppression to promote cancer metastasis. *Clin Exp Metastasis*. 2013;30:393-405.
33. Ben-Ari Z, Hochhauser E, Burstein I, et al. Role of anti-tumor necrosis factor-alpha in ischemia/reperfusion injury in isolated rat liver in a blood-free environment. *Transplantation*. 2002;73:1875-1880.
34. Mohammed FF, Smookler DS, Taylor SEM, et al. Abnormal TNF activity in Timp3-/-mice leads to chronic hepatic inflammation and failure of liver regeneration. *Nat Genet*. 2004;36:969-977.
35. Ham B, Fernandez MC, D'costa Z, Brodt P. The diverse roles of the TNF axis in cancer progression and metastasis. *Trends Cancer Res*. 2016;11:1-27.
36. Al Obeed OA, Alkhayal KA, Al Sheikh A, et al. Increased expression of tumor necrosis factor- α is associated with advanced colorectal cancer stages. *World J Gastroenterol*. 2014;20:18390-18396.
37. Grimm M, Lazariotou M, Kircher S, et al. Tumor necrosis factor-A is associated with positive lymph node status in patients with recurrence of colorectal cancer-indications for anti-TNF-A agents in cancer treatment. *Cell Oncol*. 2011;34:315-326.
38. Orosz P, Echtenacher B, Falk W, Rüschoff J, Weber D, Männel DN. Enhancement of experimental metastasis by tumor necrosis factor. *J Exp Med*. 1993;177:1391-1398.
39. Greten FR, Eckmann L, Greten TF, et al. IKK β links inflammation and tumorigenesis in a mouse model of colitis-associated cancer. *Cell*. 2004;118:285-296.
40. Pikarsky E, Porat RM, Stein I, et al. NF- κ B functions as a tumour promoter in inflammation-associated cancer. *Nature*. 2004;431:461-466.
41. Oliff A, Defeo-Jones D, Boyer M, et al. Tumors secreting human TNF/cachectin induce cachexia in mice. *Cell*. 1987;50:555-563.
42. Harrison ML, Obermueller E, Maisey NR, et al. Tumor necrosis factor alpha as a new target for renal cell carcinoma: two sequential phase II trials of infliximab at standard and high dose. *J Clin Oncol*. 2007;25:4542-4549.
43. Ham B, Wang N, D'Costa Z, et al. TNF receptor-2 facilitates an immunosuppressive microenvironment in the liver to promote the colonization and growth of hepatic metastases. *Cancer Res*. 2015;75:5235-5245.
44. Jiao S-F, Sun K, Chen X-J, et al. Inhibition of tumor necrosis factor alpha reduces the outgrowth of hepatic micrometastasis of colorectal tumors in a mouse model of liver ischemia-reperfusion injury. *J Biomed Sci*. 2014;21(1):1.
45. Ye M, Iwasaki H, Laiosa CV, et al. Hematopoietic stem cells expressing the myeloid lysozyme gene retain long-term, multilineage repopulation potential. *Immunity*. 2003;19:689-699.
46. Song Y, Shi Y, Ao LH, Harken AH, Meng XZ. TLR4 mediates LPS-induced HO-1 expression in mouse liver: role of TNF- α and IL-1 β . *World J Gastroenterol*. 2003;9:1799-1803.
47. Kirino Y, Takeno M, Murakami S, et al. Tumor necrosis factor alpha acceleration of inflammatory responses by down-regulating heme oxygenase 1 in human peripheral monocytes. *Arthritis Rheum*. 2007;56:464-475.
48. Devey L, Ferenbach D, Mohr E, et al. Tissue-resident macrophages protect the liver from ischemia-reperfusion injury via a heme oxygenase-1-dependent mechanism. *Mol Ther*. 2009;17:65-72.
49. Rossi M, Thierry A, Delbauve S, et al. Specific expression of heme oxygenase-1 by myeloid cells modulates renal ischemia-reperfusion injury. *Sci Rep*. 2017;7:197.
50. Brusko TM, Wasserfall CH, Agarwal A, Kapturczak MH, Atkinson MA. An integral role for heme oxygenase-1 and carbon monoxide in maintaining peripheral tolerance by CD4+CD25+ regulatory T cells. *J Immunol*. 2005;174:5181-5186.

SUPPORTING INFORMATION

Additional supporting information may be found online in the Supporting Information section at the end of this article.

How to cite this article: Germanova D, Keirse J, Köhler A, et al. Myeloid tumor necrosis factor and heme oxygenase-1 regulate the progression of colorectal liver metastases during hepatic ischemia-reperfusion. *Int. J. Cancer*. 2020;1-13.

<https://doi.org/10.1002/ijc.33334>